Asociación Argentina de Mecánica Computacional

Mecánica Computacional Vol XXV, pp. 2835-2850
Alberto Cardona, Norberto Nigro, Victorio Sonzogni, Mario Storti. (Eds.)
Santa Fe, Argentina, Noviembre 2006

DIRECT EVALUATION OF SINGULAR INTEGRALS IN A HOLE/INCLUSION BOUNDARY ELEMENT FOR MODELING MICRO-HETEROGENEOUS MATERIALS

Federico C. Buroni[a] & Rogério J. Marczak[b]

[a]*Department of Mechanical Engineering, Universidade Federal do Rio Grande do Sul, PROMEC-CNPq, Rua Sarmento Leite 425, 90050-170, Porto Alegre 3492, RS, Brazil, fedeburoni@yahoo.com.br, http://www-gmap.mecanica.ufrgs*

[b]*Department of Mechanical Engineering, Universidade Federal do Rio Grande do Sul, DEMEC, Rua Sarmento Leite 425, 90050-170, Porto Alegre 3492, RS, Brazil, rato@mecanica.ufrgs.br, http://www-gmap.mecanica.ufrgs*

Keywords: Micro-heterogeneous materials, boundary element method, regularization, singular integrals, direct method.

Abstract. In this work, the integration of singular kernels in a specially developed hole or inclusion boundary element is accomplished by the direct method. These elements are custom tailored for modeling two-dimensional microstructures containing cylindrical holes and/or inclusions, so that each micro-heterogeneity is represented by a single element. The traditional discretization in several boundary elements is then avoided. Using the direct method, all strongly singular integrals present in the element matrices are regularized. The convergence behavior of the proposed scheme is analyzed for several quadrature orders.

1 INTRODUCTION

The numerical integration of strongly singular kernels plays a key role in the implementation of many integral equation methods, such as the Boundary Element Method (BEM). In the last two decades, several methodologies have been proposed to perform the task. Nevertheless, only a few of them have generality for use with general fundamental tensors and higher order element shape functions. The direct method seems to be one of the most general since it imposes no formal restriction on the type of kernel to be integrated and enables the use of standard Gaussian quadrature rules (Guiggiani & Casalini, 1987; Guiggiani & Gigante, 1990). On the other hand, this method requires the knowledge of the analytical asymptotic expansions of the kernels around the singular pole. In the present work these expansions are used in the evaluation of strongly singular integrals found in a *hole/inclusion element formulation.* The hole/inclusion element is used in a special boundary element formulation (Buroni, 2006) for modeling two-dimensional microstructures containing randomly distributed cylindrical holes and inclusions.

2 BOUNDARY INTEGRAL FORMULATION

In this section, some ideas of the Boundary Element Formulation employed for numerical modeling of two-dimensional microstructure is briefly summarized. For details the reader can be consult the work of Buroni (2006).

2.1 Integrals in hole/inclusion element

A local coordinate system $\hat{x}_i$ is defined with its origin coincident with the micro-heterogeneity center. The notation "$\hat{\cdot}$" is used to refer variables in the local system. The origin of the local system in the global co-ordinate system x_i is determined by the vectors z_i, while the axis $\hat{x}_i$ are kept parallel to x_i as is indicated in Fig. 1. Thus, a particular boundary point $\hat{x}_i$ on Γ^n can be expressed as function of the angle θ according to following equation:

$$\begin{aligned} \hat{x}_1 &= R\cos\theta \\ \hat{x}_2 &= R\,\mathrm{sen}\,\theta \end{aligned} \tag{1}$$

where R is the radius of the micro-heterogeneity. The normal vectors at $\hat{x}_i$ are expressed by equation:

$$\begin{aligned} \hat{n}_1 &= -\cos\theta \\ \hat{n}_2 &= -\mathrm{sen}\,\theta \end{aligned} \tag{2}$$

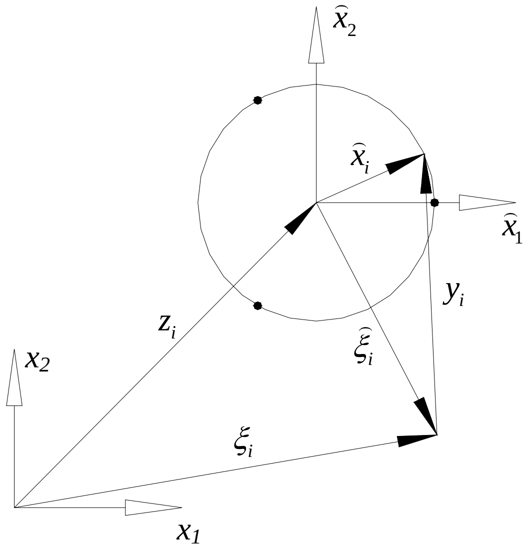

Figure 1: Local and global reference system.

In order to solve the displacement boundary integral equation of the problem it is necessary to calculate the integrals $\int_{\Gamma^n} F_{ij}\left(x,\xi\right)u_i\left(x\right)d\Gamma$ for each micro-heterogeneity boundary Γ^n, where *i,j* denote Cartesian components, u_i are the boundary displacements and F_{ij} are the components of the Kelvin fundamental solution at a point ξ due to the unit load placed at location x. These integrals are mapped to the local system and the displacement field on Γ^n is interpolated with special shape functions M_i so that each micro-heterogeneity is modeled with a single element (Buroni, 2006):

$$\int_{\Gamma^n} F_{ij}\left(x,\xi\right)u_i\left(x\right)d\Gamma = U_i^\beta \int_{2\pi}^{0} \hat{F}_{ij}\left(R,\theta,\hat{\xi}\right)M_\beta\left(\theta\right)Rd\theta \tag{3}$$

where U_i^β are the displacements of the node β in the direction *i* and β range from 1 to the number of nodes of the hole or inclusion element. Analytical expressions for the $\hat{F}_{ij}^{f}$ tensor in the reference system $\hat{x}_i$ are developed, resulting in the following expressions, valid for *plane stress* and *plane strain* hypothesis (Buroni, 2006):

$$\hat{F}_{11}\left(R,\theta,\hat{\xi}\right) = \left[\frac{C_3}{r^2\left(R,\theta,\hat{\xi}\right)}\right]\left\{\left[C_4 + \frac{2\left(R\cos\theta - \hat{\xi}_1\right)^2}{r^2\left(R,\theta,\hat{\xi}\right)}\right]\left[\hat{\xi}_1\cos\theta + \hat{\xi}_2\,\mathrm{sen}\,\theta - R\right]\right\} \tag{4}$$

$$\hat{F}_{21}\left(R,\theta,\hat{\xi}\right) =$$
$$= \left[\frac{C_3}{r^2\left(R,\theta,\hat{\xi}\right)}\right]\left\{C_4\left[\hat{\xi}_1\,\mathrm{sen}\,\theta - \hat{\xi}_2\cos\theta\right] + \left[\frac{2\left(R\cos\theta - \hat{\xi}_1\right)\left(R\,\mathrm{sen}\,\theta - \hat{\xi}_2\right)}{r^2\left(R,\theta,\hat{\xi}\right)}\right]\left[\hat{\xi}_1\cos\theta + \hat{\xi}_2\,\mathrm{sen}\,\theta - R\right]\right\} \tag{5}$$

$$\hat{F}_{12}\left(R,\theta,\hat{\xi}\right) =$$
$$= \left[\frac{C_3}{r^2\left(R,\theta,\hat{\xi}\right)}\right]\left\{C_4\left[\hat{\xi}_2\cos\theta - \hat{\xi}_1\,\mathrm{sen}\,\theta\right] + \left[\frac{2\left(R\cos\theta - \hat{\xi}_1\right)\left(R\,\mathrm{sen}\,\theta - \hat{\xi}_2\right)}{r^2\left(R,\theta,\hat{\xi}\right)}\right]\left[\hat{\xi}_1\cos\theta + \hat{\xi}_2\,\mathrm{sen}\,\theta - R\right]\right\} \tag{6}$$

$$\widehat{F}_{22}\left(R,\theta,\widehat{\xi}\right)=\left[\frac{C_3}{r^2\left(R,\theta,\widehat{\xi}\right)}\right]\left\{\left[C_4+\frac{2\left(R\,\mathrm{sen}\,\theta-\widehat{\xi}_2\right)^2}{r^2\left(R,\theta,\widehat{\xi}\right)}\right]\left[\widehat{\xi}_1\cos\theta+\widehat{\xi}_2\,\mathrm{sen}\,\theta-R\right]\right\} \tag{7}$$

where the constants C_3 and C_4 are:

$$C_3=\frac{1}{4\pi\left(1-\nu\right)} \qquad C_4=1-2\nu \tag{8}$$

and ν is the Poisson's ratio. The variable r is defined as:

$$r^2\left(R,\theta,\widehat{\xi}\right)=\left(R\cos\theta-\widehat{\xi}_1\right)^2+\left(R\,\mathrm{sen}\,\theta-\widehat{\xi}_2\right)^2 \tag{9}$$

The expressions (4)-(7) are written for plane strain hypothesis. For the plane stress case, ν must be replaced by $\overline{\nu}=\nu/(1+\nu)$.

The M_i functions are trigonometric circular functions with unitary value on the *n*-th node and zero on the others. These functions are used to interpolate both geometry and physical variables. The present formulation allows for the use of hole elements with 3, 4, 5 and 6 nodes. The 3-node element employs the functions proposed by Henry & Banerjee (1991):

$$\begin{aligned} M_1\left(\theta\right)&=\frac{1}{3}+\frac{2}{3}\cos\theta \\ M_2\left(\theta\right)&=\frac{1}{3}+\frac{\sqrt{3}}{3}\mathrm{sen}\,\theta-\frac{1}{3}\cos\theta \\ M_3\left(\theta\right)&=\frac{1}{3}-\frac{\sqrt{3}}{3}\mathrm{sen}\,\theta-\frac{1}{3}\cos\theta \end{aligned} \tag{10}$$

The shape functions of the higher order elements proposed herein are given by:

$$\begin{aligned} M_1\left(\theta\right)&=\frac{\left(1+\cos\theta\right)}{2}\cos\theta \\ M_2\left(\theta\right)&=\frac{1}{2}+\frac{1}{2}\mathrm{sen}\,\theta-\frac{1}{2}\cos^2\theta \\ M_3\left(\theta\right)&=\frac{\left(-1+\cos\theta\right)}{2}\cos\theta \\ M_4\left(\theta\right)&=\frac{1}{2}-\frac{1}{2}\mathrm{sen}\,\theta-\frac{1}{2}\cos^2\theta \end{aligned} \tag{11}$$

for the 4-node element,

$$
\begin{aligned}
M_1(\theta) &= -\frac{1}{5}+\frac{2}{5}\cos\theta+\frac{4}{5}\cos^2\theta \\
M_2(\theta) &= \frac{342}{899}\operatorname{sen}\theta+\frac{845}{1797}\operatorname{sen}\theta\cos\theta+\frac{122}{987}\cos\theta-\frac{2706}{4181}\cos^2\theta+\frac{10946}{20905} \\
M_3(\theta) &= \frac{845}{3594}\operatorname{sen}\theta-\frac{684}{899}\operatorname{sen}\theta\cos\theta-\frac{1353}{4181}\cos\theta+\frac{244}{987}\cos^2\theta+\frac{377}{4935} \\
M_4(\theta) &= -\frac{845}{3594}\operatorname{sen}\theta+\frac{684}{899}\operatorname{sen}\theta\cos\theta-\frac{1353}{4181}\cos\theta+\frac{244}{987}\cos^2\theta+\frac{377}{4935} \\
M_5(\theta) &= -\frac{342}{899}\operatorname{sen}\theta-\frac{845}{1797}\operatorname{sen}\theta\cos\theta+\frac{122}{987}\cos\theta-\frac{2706}{4181}\cos^2\theta+\frac{10946}{20905}
\end{aligned} \tag{12}
$$

for the 5-node element, and

$$
\begin{aligned}
M_1(\theta) &= -\frac{1}{6}-\frac{1}{6}\cos\theta+\frac{2}{3}\cos^2\theta+\frac{2}{3}\cos^3\theta \\
M_2(\theta) &= \frac{390}{1351}\operatorname{sen}\theta+\frac{780}{1351}\operatorname{sen}\theta\cos\theta-\frac{1}{3}\cos^2\theta-\frac{2}{3}\cos^3\theta+\frac{2}{3}\cos\theta+\frac{1}{3} \\
M_3(\theta) &= \frac{390}{1351}\operatorname{sen}\theta-\frac{780}{1351}\operatorname{sen}\theta\cos\theta-\frac{2}{3}\cos\theta-\frac{1}{3}\cos^2\theta+\frac{2}{3}\cos^3\theta+\frac{1}{3} \\
M_4(\theta) &= -\frac{1}{6}+\frac{1}{6}\cos\theta+\frac{2}{3}\cos^2\theta-\frac{2}{3}\cos^3\theta \\
M_5(\theta) &= -\frac{390}{1351}\operatorname{sen}\theta+\frac{780}{1351}\operatorname{sen}\theta\cos\theta-\frac{2}{3}\cos\theta-\frac{1}{3}\cos^2\theta+\frac{2}{3}\cos^3\theta+\frac{1}{3} \\
M_6(\theta) &= -\frac{390}{1351}\operatorname{sen}\theta-\frac{780}{1351}\operatorname{sen}\theta\cos\theta+\frac{2}{3}\cos\theta-\frac{1}{3}\cos^2\theta-\frac{2}{3}\cos^3\theta+\frac{1}{3}
\end{aligned} \tag{13}
$$

for the 6-node element.

Contrary to the conventional BEM, which requires fine meshing around each hole, the present approach allows an efficient analysis, significantly reducing the input data amount and the total number of degree of freedom without compromising the overall accuracy.

3 DIRECT EVALUATION OF STRONGLY SINGULAR KERNELS

The accuracy of the BEM for elastostatic is critically depending on the correct evaluation of boundary integrals. In this work, the integrals of the hole/inclusion element formulation are evaluated numerically using the well known Gauss-Legendre rules (Stroud & Secrest, 1966):

$$\int_{-1}^{1}\psi(x)\,dx=\sum_{i=1}^{n}w_i\psi(x_i) \tag{14}$$

where $\psi(x_i)$ is the value of the kernel evaluated on the Gauss's point x_i, and w_i are the corresponding weights for the Gauss' points. Using equation (14) implies in the mapping of the integrals (3) to a normalized space. The integrals of the fundamental solutions may present various singularity degrees, not being convenient to apply the formula (14) directly when the load point is over the element being integrated. This occurs because the integration is not convergent or presents very slow convergence. In these cases, are using special integration techniques.

The integration of equation (3) involves strongly singularities. The rigid body displacements technique is not used in this case due to its imprecision when applied to curvilinear elements (Banerjee, 1994; Guiggiani & Casalini, 1989). The work of Henry & Banerjee (1991) proposed an outer domain collocation (fictitious domain) to calculate the singular integrals of the hole element. In the present work, the integration of the strongly singular kernels is carried out by the direct method (Guiggiani & Casalini (1987), Guiggiani & Gigante (1990), Guiggiani et al. (1992) and Guiggiani (1998)). The solution of a strongly singular integral is given as a regular integral plus one scalar term evaluated on the pole.

3.1 The direct method

The formulation of the direct method is well documented in the literature. Only some basic results that are necessary throughout this work are presented here. The main goal is the accurate computation of the kernel $K_{ij}(x,\xi)=F_{ij}(x,\xi)\phi_k(x)$ over the singular element, where ϕ_k is a interpolation function of the displacement field.

Let a boundary element Γ_n be mapped into a normalized domain $\eta\subset[-1,+1]$, and $p=\eta(\xi)$ the image of the load point on the domain η (Figure 2). The general form of a strongly singular integral in the BEM can be written as follows:

$$I_{ij}=\int_{\Gamma}K_{ij}(x,\xi)\,d\Gamma=\int_{-1}^{+1}F_{ij}\left[x(\eta),\xi(p)\right]\phi_a(\eta)J(\eta)\,d\eta \tag{15}$$

where ϕ_a are the physical shape functions associated to node a and J is the determinant of the Jacobian. Hence, the kernel K_{ij} already accounts for the interpolation rule used for the physical variables on the referred boundary element. The key point in the direct method is to expand asymptotically the kernel K_{ij} using Laurent series around the image of the load point (Guiggiani, 1998):

$$\mathbf{K}(\eta,p)=\frac{\mathbf{F}_{-2}}{\rho^2}+\frac{\mathbf{F}_{-1}}{\rho}+O(1) \tag{16}$$

where $\rho=\eta-p$ is the image of r in the normalized domain. The expansion $\mathbf{F}_{-1}$ accounts for the strongly singular contributions of the kernel, while the expansion $\mathbf{F}_{-2}$ accounts for the hypersingular contributions and so forth. Higher order singularities can be considered increasing the quantity of terms in the series. Then, a regular or weakly singular kernel has $\mathbf{F}_{-1}=\mathbf{F}_{-2}=0$. The expansion $\mathbf{F}_{-2}$ vanishes in the case of a strongly singular kernel, but not for hypersingular kernels.

When the collocation point lies within only one boundary element, the final formula of the direct method is given by (Guiggiani, 1998):

$$\begin{aligned}I=\int_{-1}^{+1}\left[\mathbf{K}(\eta,p)-\left(\frac{\mathbf{F}_{-1}}{\rho}+\frac{\mathbf{F}_{-2}}{\rho^2}\right)\right]d\eta+\mathbf{F}_{-1}(\eta)\ln\left|\frac{1-\eta}{-1-\eta}\right|+\\+\mathbf{F}_{-2}(\eta)\left(-\frac{1}{1-\eta}+\frac{1}{-1-\eta}\right)\end{aligned} \tag{17}$$

One should note that the expression (17) contains all the information regarding the shape functions used for the physical variables (ϕ_a) and geometry (J) enabling a rather general application. The integral in (17) stands for the original kernel from which the singular part around the load point has been subtracted, resulting in a regular integral. Another two terms in equation (17) correspond to analytical integration of the singularity through a criteriously limit process (Guiggiani, 1998). Then, the singular integral is obtained as a regular integral plus two scalar terms evaluated in the pole. The derivation of the expression (17) does not have any approximation in relation to the original integral (15). Thus, the generic application of the direct method implies only in the knowledge of the expansions $\mathbf{F}_{-1}$ and $\mathbf{F}_{-2}$ for equation (16).

For the case of two-dimensional elasticity, Marczak & Creus (2002) have derived a general expression for the Laurent's expansion $\mathbf{F}_{-1}$ and $\mathbf{F}_{-2}$ obtaining:

$$F_{-1}^{\alpha\beta} = -\frac{(1-2\nu)}{4\pi(1-\nu)}\left[n_\alpha(\xi)t_\beta(\xi)-n_\beta(\xi)t_\alpha(\xi)\right]\phi_a(p)$$
$$F_{-2}^{\alpha\beta} = 0 \tag{18}$$

where n_α and t_α are the normal and tangential vector on the point ξ respectively. It is interesting to note in equation (18) that only the off-diagonal terms are strongly singular while in the diagonal ones ($\alpha=\beta$) $\mathbf{F}_{-1}=\mathbf{F}_{-2}=0$, which means that the integral is regular (contrary to what can be suggested by the expressions (4) and (7)). That is, the simple presence of r in the denominator of a fundamental solution must not be taken as a sufficiency condition to qualify a kernel as strongly singular (Marczak & Creus, 2002). Also observed from equation (18) is the necessity of taking into account the asymptotic behavior of the whole kernel, including the interpolation function (ϕ_a) and the determinant of the Jacobian (J) (Marczak & Creus, 2002). In the studied case, the interpolation functions used to approximate the displacement fields in the hole have unitary value in the referring node and zero in the others. This means that only the integrals containing non-null shape functions on the image of the collocation node are strongly singular.

3.2 Laurent's expansions for the hole/inclusion element

In order to found the functions $\mathbf{F}_{-1}$ and $\mathbf{F}_{-2}$ in a systematic manner for the hole and inclusion elements some useful relations of the normal and tangential vectors are presented (Marczak & Creus, 2002):

$$n_i = \frac{J_i}{J} \tag{19}$$

$$t_i = \frac{A_i}{J} \tag{20}$$

The determinant of the Jacobian can be expanded in Taylor series as:

$$J = \sqrt{\frac{dx_\alpha}{d\eta}\frac{dx_\alpha}{d\eta}} = \sqrt{J_1(\eta)^2 + J_2(\eta)^2} \tag{21}$$

where

$$J_1 = A_2 + 2B_2\rho + O\left(\rho^2\right) \tag{22}$$

$$J_2 = -A_1 - 2B_1\rho + O\left(\rho^2\right) \tag{23}$$

and

$$A_i = \left.\frac{dx_i}{d\eta}\right|_{\eta=p} \tag{24}$$

$$B_i = \frac{1}{2}\left.\frac{d^2x_i}{d\eta^2}\right|_{\eta=p} \tag{25}$$

The boundary Γ_n is mapped to a normalized space $\eta \subset [-1,+1]$ with the following transformation:

$$\lambda + \theta = (\eta + 1)\pi \tag{26}$$

Note that λ could have any value, but if this value is zero it happens a particular situation where the collocation point is the node 1 (see Figure 2). Since the element is closed, this point presents double-pole singularity (on $\eta = -1$ and $\eta = 1$), corresponding to the angles $\theta = 0$ and $\theta = 2\pi$, respectively. The direct method is not able to eliminate both singularities simultaneously, so the parameter λ must be different to zero. It is proposed the mapping (26) with $\lambda = \frac{1}{3}\pi$, $\lambda = \frac{1}{4}\pi$, $\lambda = \frac{1}{5}\pi$ and $\lambda = \frac{1}{6}\pi$ for the 3, 4 ,5 and 6-node element respectively. Thus the poles are displaced by λ/π as is showed in Figure 2.

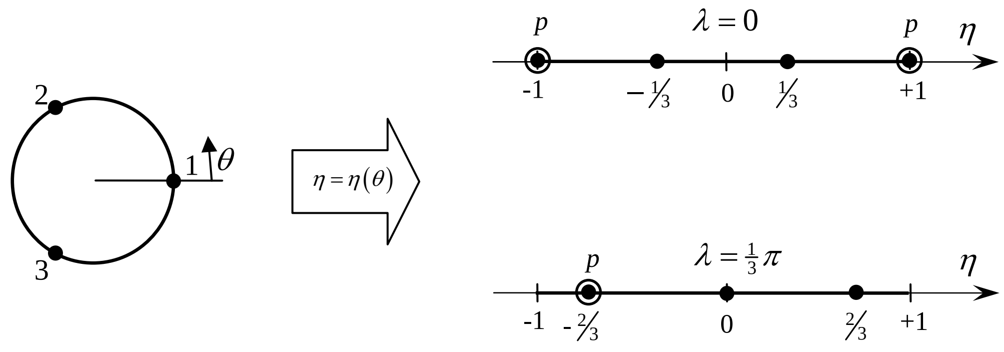

Figure 2: Mapping of the 3-node element to the normalized space η with $\lambda = 0$ and $\lambda = \frac{1}{3}\pi$.

Taking into account this mapping and the geometry in the system $\hat{x}_i$, the expressions (19)-(25) are particularized to the form:

$$A_1 = \left.\frac{d\hat{x}_1}{d\theta}\frac{d\theta}{d\eta}\right|_{\eta=p} = -R\pi \operatorname{sen}\theta\Big|_{\eta=p} \tag{27}$$

$$A_2 = \left.\frac{d\hat{x}_2}{d\theta}\frac{d\theta}{d\eta}\right|_{\eta=p} = R\pi \cos\theta\Big|_{\eta=p} \tag{28}$$

$$B_1 = B_2 = 0 \tag{29}$$

$$J_1 = R\pi \cos\theta \tag{30}$$

$$J_2 = R\pi \operatorname{sen}\theta \tag{31}$$

Neglecting the high order terms:

$$J = \sqrt{\left(R\pi\cos\theta\right)^2 + \left(R\pi \operatorname{sen}\theta\right)^2} = R\pi \tag{32}$$

With these expressions the equations (19) and (20) became:

$$\begin{aligned} t_1 &= -\operatorname{sen}\theta \\ t_2 &= \cos\theta \end{aligned} \tag{33}$$

$$\begin{aligned} n_1 &= \cos\theta \\ n_2 &= \operatorname{sen}\theta \end{aligned} \tag{34}$$

Finally the terms in the Laurent's expansion (equation (18)) which regularize the integrals for the hole or inclusion element result:

$$F_{-1}^{12} = -\frac{(1-2\nu)}{4\pi(1-\nu)} M_a(p) \tag{35}$$

$$F_{-1}^{21} = \frac{(1-2\nu)}{4\pi(1-\nu)} M_a(p) \tag{36}$$

It worth noting that the mapping (26) used in this deduction implies that the direction of travel on the boundary Γ_n is counterclockwise (corresponding to external normal of the inclusion domain). However, the expressions (35) and (36) remain the same if the element orientation is clockwise (corresponding to external normal of the matrix domain).

One should also note that the direct method allows the regularization of the strongly singular contribution only, with the visualization of the kernels helping to verify the overall behavior of the regularized kernels.

4 NUMERICAL EXPERIMENTS

In order to provide a verification of the efficiency of the integration for the proposed hole/inclusion element some numerical experiments are presented in this section. Figures 3 and 4 show the singular behavior of the functions $F_{12}M_1J$ and $F_{21}M_1J$ in the normalized space when collocation is performed on the $\left(\hat{\xi}_1, \hat{\xi}_2\right) = \left(R, 0\right)$ co-ordinates. In these figures the effect of the regularization of the kernels as well as the asymptotic expansions can be visualized. The regular integral (see equation (17)) is calculated with the standard Gauss-Legendre quadrature technique using K points. The effectiveness of the proposed integration technique can be examined in the Table 1 where results for all singular integral in the 3-node hole element are presented.

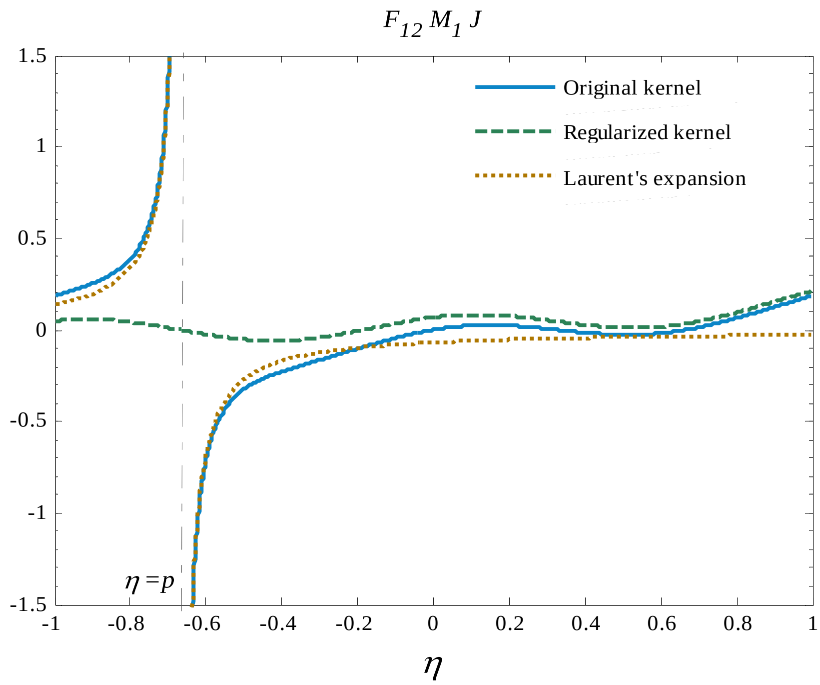

Figure 3: Behavior of $F_{12}M_1J$ on normalized space η when collocation is doing on $\hat{\xi}_1 = R$ and $\hat{\xi}_2 = 0$ co-ordinates (3-node hole element).

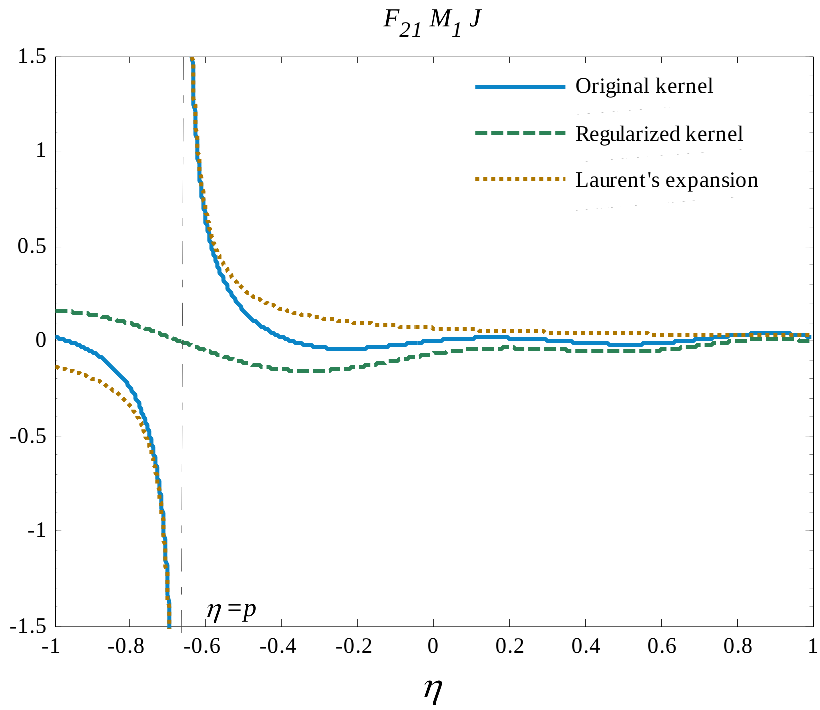

Figure 4: Behavior of $F_{21}M_1J$ on normalized space η when collocation is doing on $\hat{\xi}_1 = R$ and $\hat{\xi}_2 = 0$ co-ordinates (3-node hole element).

K	$\int_{-1}^{+1} F_{12} M_1 J \, d\eta$	$\int_{-1}^{+1} F_{21} M_1 J \, d\eta$	$\int_{-1}^{+1} F_{12} M_2 J \, d\eta$	$\int_{-1}^{+1} F_{21} M_2 J \, d\eta$	$\int_{-1}^{+1} F_{12} M_3 J \, d\eta$	$\int_{-1}^{+1} F_{21} M_3 J \, d\eta$
2	-0,0906830057	-0,0420223859	-0,0128691349	-0,0128691349	-0,1699279990	-0,2185886188
4	-0,0100886758	-0,0120556646	0,0954351670	0,0954351670	-0,1134493895	-0,1114824007
6	-0,0001553394	-0,0001378292	0,1029515549	0,1029515549	-0,1032361530	-0,1032536637
8	-0,0000007553	-0,0000000219	0,1030978737	0,1030978737	-0,1030982842	-0,1030990176
10	-0,0000000153	0,0000000145	0,1030982620	0,1030982620	-0,1030982477	-0,1030982776
16	0	0	0,1030982623	0,1030982623	-0,1030982622	-0,1030982624

Table 1: Results of the singular integrals of the 3-nodes hole element with the direct method. The variable K is referred to the number of Gauss – Legendre points.

The method of collocation over a fictitious boundary proposed by Henry & Banerjee (1991) to evaluate the singular integral is now analyzed for the present 3-node hole element. Figure 5 shows the kernel $F_{12}M_1J$ in the normalized space with $\left(\hat{\xi}_1,\hat{\xi}_2\right)=\left(\hat{\xi}_1,0\right)$. Note that this integral is singular when $\hat{\xi}_1 = R$ (see Figure 3). In Figure 5 one can be observe that using the collocation on the fictitious boundary the integral becomes regular, as expected, although becoming less smooth as the collocation point approaches the boundary of the hole element. This behavior is also observed in the Figures 6 and 7, revealing a difficult numerical integration. Table 2 presents the integrals $\int_{-1}^{+1} F_{12} M_1 J \, d\eta$ in the normalized space η for the 3-node hole element with collocation on $\left(\hat{\xi}_1,\hat{\xi}_2\right)=\left(\hat{\xi}_1,0\right)$ by the standard Gauss-Legendre quadrature technique using K points. The row **M** refers to the integration performed with Maple (2003) program, which uses more efficient integration techniques. These results reveal that in the present case Gauss-Legendre quadrature is not convenient when collocation is carried on a fictitious boundary. It is worth to mention that in the work of Henry & Banerjee (1991) the collocation is carried on a fictitious boundary with radius 25% smaller than the hole.

As can be deduced from the direct method, the kernel $F_{22}M_1J$ is regular because F_{22} is a diagonal term, and the kernel $F_{21}M_3J$ is also regular since the shape function M_3 becomes null when it is evaluated on the pole (see equation (18)). However, Figures 6 and 7 show that the collocation on a fictitious boundary turn these kernels less smooth, and more difficult to integrate. According to the results shown in Tables 3 and 4, while these integrals are easily evaluated with 8 Gauss points, in many cases 64 points are not sufficient when the collocation is performed on a fictitious boundary.

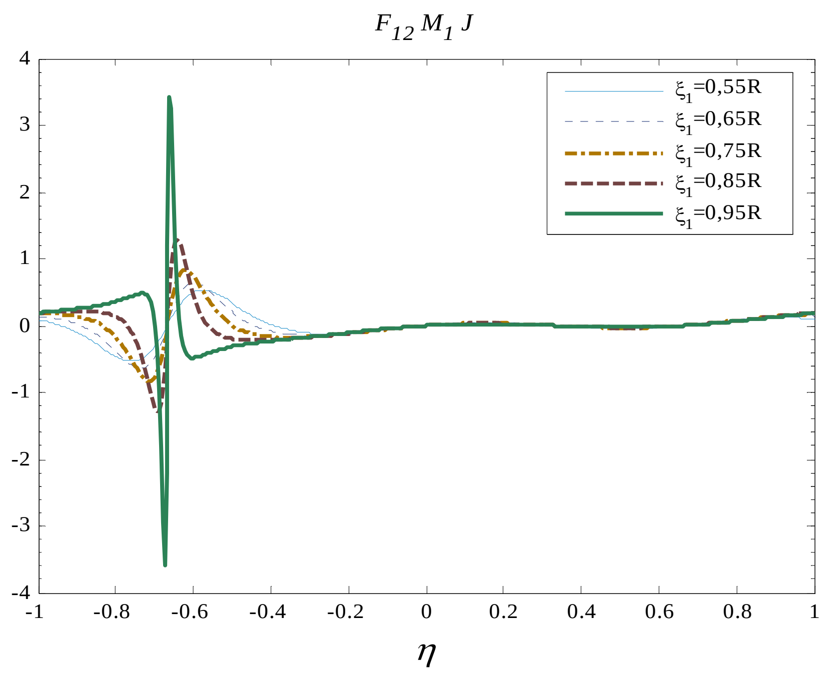

Figure 5: Kernel $F_{12}M_1J$ on the normalized space η when collocation is doing on $\hat{\xi}_1$ and $\hat{\xi}_2 = 0$ co-ordinates (3-nodes hole element).

	$\int_{-1}^{+1} F_{12}M_1J\, d\eta$				
K	$\hat{\xi}_1 = 0,55$	$\hat{\xi}_1 = 0,65$	$\hat{\xi}_1 = 0,75$	$\hat{\xi}_1 = 0,85$	$\hat{\xi}_1 = 0,95$
2	0,4996274853	0,5735158877	0,5068130807	0,1009152246	-0,4689180337
4	-0,1002672434	-0,0832486298	-0,0466133316	-0,00851649	0,0132779673
6	-0,0069769269	0,0182694658	0,0592049376	0,1673348176	1,1397498933
8	0,0270281486	0,0223166112	0,0089186448	-0,0040539271	-0,00923141485
10	-0,0255006629	-0,0466853398	-0,0868154614	-0,2072715589	-0,674246733
16	0,0000000008	-0,000000211	-0,0000754613	-0,0065360969	-0,1558334228
20	0,0004056231	0,0047222951	0,0308300392	0,1206006627	0,0536906454
24	0,0000122533	0,0008807299	0,0118965367	0,0844295122	0,1942318955
32	-0,0000022819	-0,0000467012	-0,0000028392	0,0097769609	0,1747858787
40	-0,0000000354	-0,0000073850	-0,0004063562	-0,010461151	-0,1797103976
48	0,0000000008	0,0000000008	-0,0000754613	-0,0065360969	-0,1558334228
64	0	0,0000000001	0,0000016898	0,0003037949	0,0094003974
M	0	0	0	0	0

Table 2: Results of integrals $\int_{-1}^{+1} F_{12}M_1J\, d\eta$ for the 3-nodes hole element with collocation on $\hat{\xi}_1$ and $\hat{\xi}_2 = 0$ by the standard Gauss-Legendre quadrature technique with points K points.

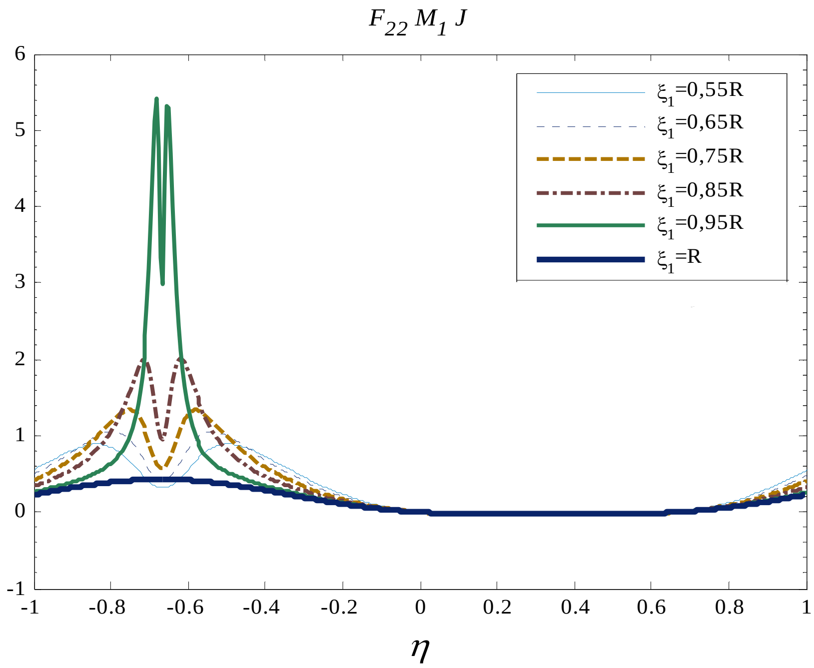

Figure 6: Kernel $F_{22}M_1J$ on the normalized space η when collocation is doing on $\hat{\xi}_1$ and $\hat{\xi}_2 = 0$ co-ordinates (3-nodes hole element).

$\int_{-1}^{+1} F_{22}M_1J\, d\eta$						
K	$\hat{\xi}_1 = 0,55R$	$\hat{\xi}_1 = 0,65R$	$\hat{\xi}_1 = 0,75R$	$\hat{\xi}_1 = 0,85R$	$\hat{\xi}_1 = 0,95R$	$\hat{\xi}_1 = R$
2	0,6544569211	0,9415202291	1,3124938877	1,500233656	0,9272763187	0,3927711795
4	0,7157020404	0,6803904348	0,6016911575	0,4845903435	0,3512584301	0,2873830534
6	0,4358738207	0,4334965656	0,4513181780	0,5567690033	1,5722486092	0,2857990867
8	0,6485691854	0,7280318858	0,7570033652	0,6596240653	0,4230954335	0,2857145100
10	0,5548558685	0,5598308865	0,5510520606	0,5941668872	1,4174691308	0,2857142859
16	0,5821428582	0,6273813806	0,6726505367	0,7180423354	0,7849876626	0,2857142857
20	0,5817657263	0,6259344381	0,6717446408	0,7390321328	0,7704249468	0,2857142857
24	0,5820524686	0,6263580410	0,6662137031	0,6989334415	0,8793821755	0,2857142857
32	0,5821419504	0,6272907099	0,6701842342	0,6870751694	0,6738938507	0,2857142857
40	0,5821429032	0,6273809527	0,6723746529	0,7071040271	0,7007284870	0,2857142857
48	0,5821428582	0,6273813806	0,6726505367	0,7180423354	0,7849876626	0,2857142857
64	0,5821428572	0,6273809520	0,6726204717	0,7186825791	0,8193213854	0,2857142857
M	0,5821428572	0,6273809525	0,6726190477	0,7178571430	0,7630952382	0,2857142858

Table 3: Results of integrals $\int_{-1}^{+1} F_{22}M_1J\, d\eta$ for the 3-nodes hole element with collocation on $\hat{\xi}_1$ and $\hat{\xi}_2 = 0$ by the standard Gauss-Legendre quadrature technique with points K points.

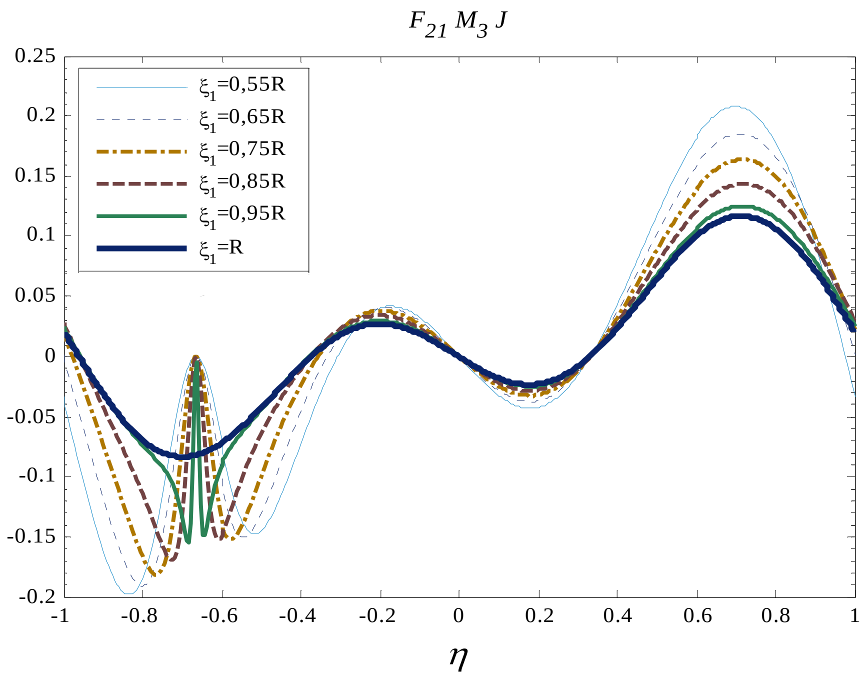

Figure 7: Kernel $F_{21}M_3J$ on the normalized space η when collocation is doing on $\hat{\xi}_1$ and $\hat{\xi}_2 = 0$ co-ordinates (3-nodes hole element).

$\int_{-1}^{+1} F_{21}M_3J\,d\eta$						
K	$\hat{\xi}_1 = 0,55R$	$\hat{\xi}_1 = 0,65R$	$\hat{\xi}_1 = 0,75R$	$\hat{\xi}_1 = 0,85R$	$\hat{\xi}_1 = 0,95R$	$\hat{\xi}_1 = R$
2	0,0633211216	0,0132709361	-0,0234557166	-0,0171949043	0,0223215849	0,0255811226
4	-0,0311281851	-0,0085957102	0,01154883782	0,0238127932	0,0242360241	0,0202787449
6	0,0590163752	0,0649659139	0,0658870503	0,0607482422	0,0380897305	0,0206196647
8	-0,0110969181	-0,0130757548	-0,0043853567	0,0132490408	0,0232252332	0,0206196524
10	0,0211723316	0,0313640255	0,0399001428	0,04005423308	0,0138006206	0,0206196524
16	0,0113408084	0,0134026753	0,0154602646	0,01752666859	0,0188876608	0,0206196524
20	0,0114449175	0,0136551751	0,0153835071	0,01516896084	0,0169477101	0,0206196524
24	0,0113696751	0,0136340597	0,0164836958	0,01968690216	0,0163524927	0,0206196524
32	0,0113412171	0,0134260660	0,0158839898	0,02083706671	0,0267519208	0,0206196524
40	0,0113407956	0,0134029664	0,0155107639	0,01867844978	0,0238278769	0,0206196524
48	0,0113408084	0,0134026757	0,01546026469	0,01752666859	0,0188876608	0,0206196524
64	0,0113408088	0,0134027741	0,0154644804	0,017443313	0,0170441945	0,0206196524
M	0,0113408088	0,01340277411	0,01546473936	0,01752670461	0,0195886698	0,0206196524

Table 4: Results of integrals $\int_{-1}^{+1} F_{21}M_3J\,d\eta$ for the 3-nodes hole element with collocation on $\hat{\xi}_1$ and $\hat{\xi}_2 = 0$ by the standard Gauss-Legendre quadrature technique with points K points.

5 CONCLUSIONS

The integration of strongly singular integrals in a hole and inclusion element have been accomplished by the direct method, resulting in a regularized element. A critical study of the direct method allows recognizing in integrals of the form $\int_{-1}^{+1} F_{ij}\left[x(\eta),\xi(p)\right]\phi_a(\eta)J(\eta)d\eta$ which ones are effectively singular. The analytic expressions for the terms $\mathbf{F}_{-1}$ of the Laurent's expansion have been derived in a systematic manner, which is the main result of this work. These terms are valid for both hole and inclusion elements, regardless the order of the element shape functions. The numerical experiments have shown that the regularized integrals can be evaluated effectively by standard Gauss-Legendre quadrature rules. Another way of avoid the singularity is to perform the collocation on a fictitious boundary. However, the kernels become less smooth and much more difficult to integrate when the load point is approaching to the element.

ACKNOWLEDGEMENTS

The first author wishes to express his thanks to CNPq for the financial support and is also grateful to Prof. Adrián P. Cisilino for very useful discussions. This work was partially financed by PROSUL 490185/2005-3 and CAPES/SETCIP 048/03 projects.

REFERENCES

P. K. Banerjee. *The Boundary Element Methods in Engineering*. Mc Graw-Hill Book Company, 1994.

F. C. Buroni. Modelagem e Projeto Computacional de Materiais Micro-Porosos com Distribuição Aleatória Utilizando uma Formulação de Elementos de Contorno. Master thesis, Universidade Federal de Rio Grande do Sul, Porto Alegre, Brazil, 2006.

C. A. Brebbia & J. Dominguez. *Boundary Elements. An Introductory Course*. Second Edition. Computational Mechanics Publications. Southampton Boston – Mc Graw-Hill Book Company, 1992.

M. Guiggiani. *Formulation and Numerical Treatment of Boundary Integral Equations with Hypersingular Kernels*. V. Sladek and J Sladek, eds. Singular Integrals in B. E. Methods, Computational Mechanics Publications, Chapter 3, pp. 85-124, 1998.

M. Guiggiani & P. Casalini. Direct Computation of Cauchy Principal Value Integrals in Advanced Boundary Elements. *International Journal of Numerical Methods in Engineering*. vol. 24, pp. 1711-1720, 1987.

M. Guiggiani & P. Casalini. Rigid –body Translation with Curved Boundary Elements. *Applied Mathematical Modeling*. vol. 13, pp. 365-368, 1989.

M. Guiggiani & A. Gigante. A General Algorithm for Multidimensional Cauchy Principal Value Integrals in the Boundary Element Method. *Journal of Applied Mechanics*, vol. 57, pp. 906-915, 1990.

M. Guiggiani, G. Krishnasamy, T. J. Rudolphi & F. J. Rizzo. A General Algorithm for the Numerical Solution of Hypersingular Boundary Integral Equations. *Journal of Applied Mechanics*, vol. 59, pp. 604-614, 1992.

D. P. Henry & P. K. Banerjee. Elastic Stress Analysis of Three-Dimensional Solids with Small Holes by BEM. *International Journal for Numerical Methods in Engineering*, vol. 31, pp. 369–384, 1991.

Maple. *User's Guide version 9.01*. The Maplesoft, Waterloo Maple Inc, 2003.

R. J. Marczak & G. J. Creus. Direct Evaluation of Singular Integrals in Boundary Element Analysis of Thick Plates. *Engineering Analysis with Boundary Elements*, vol. 26, pp. 653–665, 2002.

A. H. Stroud & D. Secrest. *Gaussian Quadrature Formulas*, Prentice-Hall, 1966.